www.czasopisma.pan.pl PAN POLSKA AKADEMIA NAUK www.journals.pan.pl

A R C H I V E S O F M E T A L L U R G Y A N D M A T E R I A L S

Volume 60 2015 Issue 2

DOI: 10.1515/amm-2015-0103

S.-Y. KIM*, M.-H. LEE*, T.-S. KIM*, B.-S. KIM*,#

CO OXIDATION PROPERTIES OF SELECTIVE DISSOLUTED METALLIC GLASS COMPOSITES

UTLENIANIE WYBRANYCH ROZCIEŃCZONYCH KOMPOZYTÓW SZKIEŁ METALICZNYCH

Porous metallic materials have been widely used in many fields including aerospace, atomic energy, electro chemistry and environmental protection. Their unique structures make them very useful as lightweight structural materials, fluid filters, porous electrodes and catalyst supports. In this study, we fabricated Ni-based porous metallic glasses having uniformly dispersed micro meter pores by the sequential processes of ball-milling and chemical dissolution method. We investigated the application of our porous metal supported for Pt catalyst. The oxidation test was performed in an atmosphere of 1% CO and 3% O_2. Microstructure observation was performed by using a scanning electron microscope. Oxidation properties and BET (Brunauer, Emmett, and Teller) were analyzed to understand porous structure developments. The results indicated that CO Oxidation reaction was dependent on the specific surface area.

Keywords: CO Oxidation, metallic gasses, Porous metal, catalyst materials

1. Introduction

Porous metal is a material with countless small cells that are regularly or irregularly dispersed inside. Porous metallic materials have been widely used in many fields including aerospace, atomic energy, electro chemistry and environmental protection [1-3]. Amorphous materials have a variety of advantages such as large elastic limit, wear resistance and random packing of atoms. This class of materials has many promising properties, e.g., extremely high strength and hardness combined with relatively high fracture toughness, as well as good wear and corrosion resistance [4-10]. Therefore, porous amorphous materials combined with materials have many advantages [11-14]. Their unique structures make them very useful as lightweight structural materials, fluid filters, separation membranes, porous electrodes, impact energy absorbers, heat exchangers and catalyst supports [15-18]. In addition, porous metals can be used as filters due to their larger surface area, which further accelerates the expansion of their increasingly widening scope of applicability over recent years. As a filter material, porous metals are known to further improve the part's filtering ability if the size of the pores is smaller, since finer pores increase the area that absorbs pollutants. To date, porous metals have largely been fabricated from various elemental and intermetallic systems using a variety of processing routes [19-26]. In this study, metallic glass foams were fabricated by ball milling powder mixtures comprised of metallic glasses and fugitive phases followed by dissolution of the fugitive phases in chemical solution to yield the final porous structure. Also, we performed an oxidation test to apply the supported catalyst to investigate CO activation. In addition, a study of the relationship between the oxidation and specific surface area (by BET (Brunauer, Emmett and Teller) was conducted.

2. Experimental

To synthesize $Ni_{59}Zr_{20}Ti_{16}Si_2Sn_3$ amorphous powder using high pressure gas atomization process, the master alloy prepared by vacuum plasma melting was re-melted by a vacuum induction furnace in the gas atomization system. To make the composite powders, milling of the Ni-based amorphous powder blended with 40 vol % brass powders was perfor8med in a glove box using a planetary mill at a rotation velocity of 150 rpm for 20 h using hardened steel milling tools and a ball to powder ratio of 10:1. The dissolved powder was extracted through a filter and rinsed eight to ten times to separate it from the 20% HNO_3 aqueous solutions. The obtained composite powder (4 g) was dissolved in 20% aqueous HNO_3 solutions with increasing time at room temperature. The weight loss with increasing dissolution time of the dissolved powder was measured. Ni-based amorphous porous powder was used to prepare supported Pt catalysts. Activity maintenance profiles for CO oxidation over the Ni-based porous metal/pt catalysts under the chosen conditions were measured using a gas phase continuous flow U-shaped Pyrex reactor in a tubular electric furnace coupled with a Hanyaoung Model NP200 PID temperature controller. An appropriate amount of the catalyst (0.2g) was placed above a quartz wool plug in the Pyrex reactor

* KOREA INSTITUTE FOR RARE METALS, KOREA INSTITUTE OF INDUSTRIAL TECHNOLOGY,7-47 SONGDO DONG, YEONSOO GU, INCHEON 406-840, KOREA

Corresponding author: bskim15@kitech.re.kr

and routinely calcined unless otherwise specified at 350° for 1h in a flow of simulated air at 200 ml/min using a Brooks 5850E Mass Flow Controller (MFC) before the CO oxidation reaction was allowed with the reaction parameter chosen here. A gas mixture consisting of 1% CO and 3% O_2 in flowing He at a total flow rate of 200cm^3/min, corresponding to gas hourly space velocities (GHSV) of 64,500 h^{-1}, was passed continuously through the catalyst bed for CO oxidation at the given reaction temperatures. Microstructure characterization was performed using a scanning electron microscope (SEM). The specific surface area of the porous powder was determined using the Brunauer–Emmett–Teller (BET) method (Adsotrac DN-04).

3. Results and discussion

The $Ni_{59}Zr_{20}Ti_{16}Si_2Sn_3$ (in atomic percentage) metallic glass powders used in this study were prepared by the high pressure gas atomization method. In this work, Ni-based composite powder was fabricated by ball milling of two different mixtures of powders consisting of brass. Figure 1 show optical micrographs of the Ni-based composite powder on cross section. The microstructure represents a layered structure resulting in the intermediate mixing between Ni-based metallic glass and fugitive phase by call milling. The dark gray area indicated an MG (Metallic Glass) phase and the yellow area is brass. The brass powders are well elongated along the milling direction in the metallic glass matrix. Small particles display a microstructure consisting of alternate layers of brass and glass.

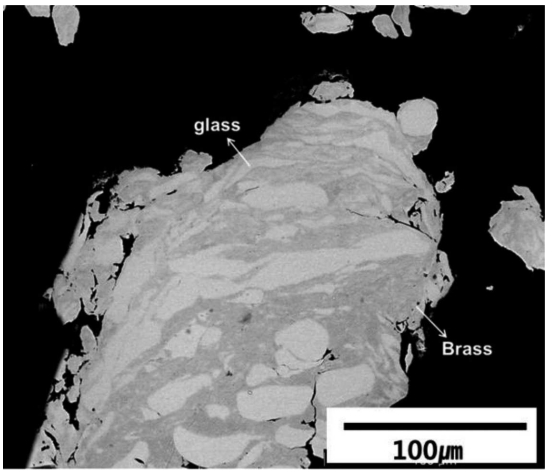

Fig. 1. Cross sectional image of Ni-based metallic glass powders

Investigation of the properties of CO oxidation reaction for porous materials fabricated in this study and the catalyst activity using Pt catalyst with time variables are shown in Figure 2. The Pt catalyst used as active materials has an advantage to oxidation reaction of CO because the precious metals such as Pt have relatively high electron density compared with other materials. From the results, porous materials in 5 conditions have similar tri-step CO reaction behavior. In the first step, CO conversion gradually appeared as increasing time and CO reaction was rapidly converted in the second step. In the third step, the oxide reaction behavior was girdled. T50 of the specimen dissolved for 1h was 214.7°, which was the lowest value. Subsequently, T50 was increased with increases in time and 360.5° was measured as the highest T50 for 12h. This result showed that the specific surface area was changed by flow and that the CO transition at low temperature has excellent properties.

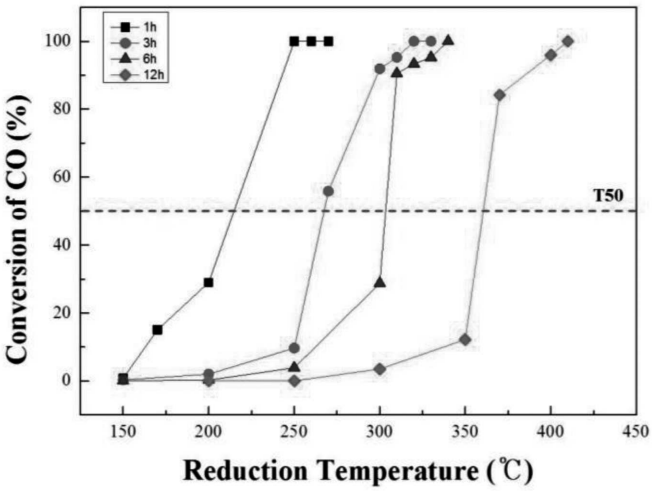

Fig. 2. Conversion of CO vs. Reduction temperature of Ni-based porous powders

Figure 3 shows the Ni-based porous powder microstructure image with dissolution time in 20% HNO_3. Overall, the pore size gradually decreases with increasing chemical reaction time. (a) is powder dissolved for 1 hour. As a result, the brass that forms a layer in the Ni-rich phase has been removed and an elongated structure of powder is observed. (b) Ni-rich phase was maintained layer-shape. After dissolving for 6 hours(c) a smooth-surfaced powder was observed with the dissolution time variables. In figure (d), the specimen that was dissolved for 12 hours shows a smooth surface and small particle sizes.

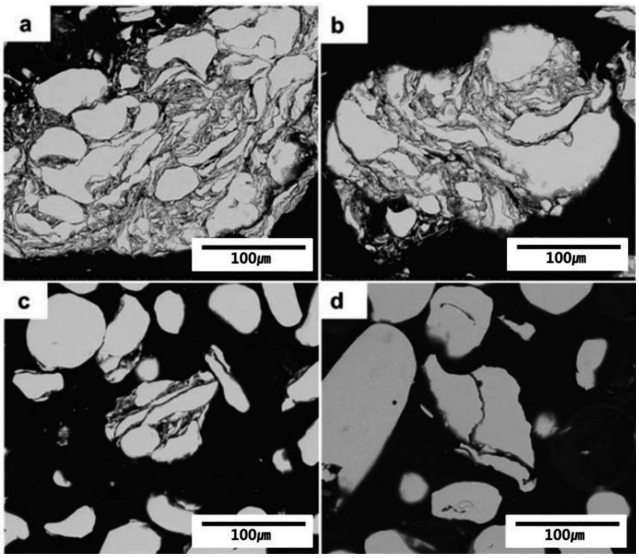

Fig. 3. SEM backscattered electron images obtained from the polished cross section of the porous powder;(a)1h, (b)3h, (c) 6h, (d) 12h

Figure 4 showed the relative specific surface area results of measured porous powder and the temperature of T50 with

the dissolution time. The 1-hour dissolution shows the highest specific surface area of 1, and sharply decreases to the value of 0.1 (10%) after 12 hours. This result agrees with figure 4 (T50) dissolution time-based T50 temperature changes. T50 is a base temperature where CO oxidizes into CO_2; and where the lower the reaction temperature, the more active the catalytic activity [27]. The temperature of the best activity of T50 at 214° is one hour using the dissolution powder with the highest specific surface area. A greater time of dissolution yields higher T50 temperatures and lower oxidation activity. The powder dissolved for 1 hour has the highest specific surface area, a roughened shape with the pore formed by brass dissolution inside composites. As dissolution time increases, the Ni-rich phase reacts and the surface developed a smooth shape with nitric acid because the interior brass nearly disappears. Also, the initial aggregated shape was destroyed resulting in a smooth-surfaced, small size and limited foaming inside the pore. Therefore, the specific surface area was decreased. Based on the results, CO activity emerges depending on the specific surface area, and the more specific surface area, the lower the temperature of oxidization activity.

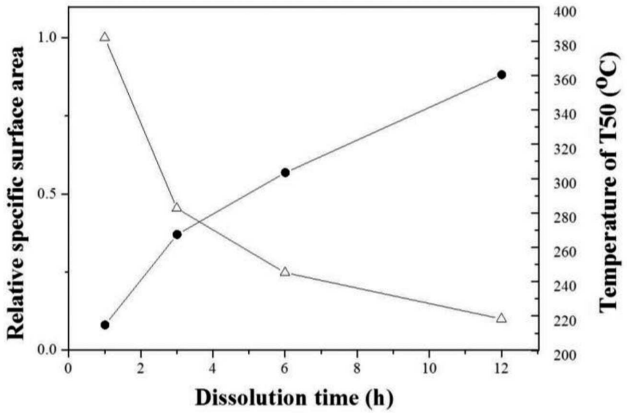

Fig. 4. Relative specific surface area and temperature of T50 vs. dissolution time

4. Conclusions

This study investigated the CO oxidation activity of Ni-based MG porous with dissolution time. CO Oxidation tests of fabricated porous MG were progressed to examine the possibility of a catalyst supported application. Based on the results of the CO oxidation testing, the following conclusions were obtained:

A Ni-based porous MG has been fabricated by applying the chemical dissolution method. As CO oxidation results, T50 temperature is 214.7°, which is the minimum value at dissolution for 1 hour. With increasing dissolution time, the T50 temperature tended to increase but slightly decreased at dissolution for 12 hours. In the case of BET results, the relative specific surface area is 1, which is the maximum value at dissolution for 1 hour. With increasing dissolution time, the specific surface area tended to decrease. The relationship between the specific surface area and T50 temperature showed a linear result. The specific surface area values decrease with decreasing T 50 temperature (high activity)

REFERENCES

[1] P.S. Liu, K.M. Liang, J Mater Sci. **36**, 5059 (2001).
[2] A.H. Brothers, D.C. Dunand. Scripta Mater. **54**, 513 (2006).
[3] S.Y. Kim, B.K. Guem, M.H. Lee, T.S. Kim, E. Jurgen, B.S. Kim, J Kor Powd Met Inst. **21**, 251 (2014).
[4] H.A. Bruck, T. Christman, A.J. Rosakis, W.L. Johnson, Scr. Metall. Mater. **30**, 429 (1994).
[5] R.D. Conner, A.J. Rosakis, W.L. Johnson, D.M. Owen, Scr. Mater. **37**, 1373 (1997).
[6] C.J. Gilbert, R.O. Ritchie, W.L. Johnson, Appl. Phys. Lett. **71**, 476 (1997).
[7] M.Z. Ma, R.P. Liu, Y. Xiao, D.C. Lou, L. Liu, Q.Wang, W. K.Wang, Mater. Sci. Eng. A. **386**, 326 (2004).
[8] J. Jayaraj, D.J. Sordelet, D.H. Kim, Y.C. Kim, E. Fleury, Corros. Sci. **48**, 950 (2006).
[9] E.S. Park, H.K. Lim, W.T. Kim, D.H. Kim, J.Non-Crys Solids **298**, 15 (2002).
[10] J.S. Kim, M.H. Lee, D.H. Kim, U. Kühn and J. Eckert, Revue de Métallurgie. **109**, 11 (2012).
[11] G. He, J. Eckert, W. Loeser, Acta Mater. **51**, 1621 (2003)
[12] J.K. Lee, H.J. Kim, M. Yamasaki, Y. Kawamura, J. C. Bae, Mater. Sci. Forum, **475-479**, 3419 (2005).
[13] H. Kato, K. Yubuta, D.V. Louzguine, A. Inoue, H.S. Kim, Scripta Mater. **51**, 577 (2004).
[14] T.S. Kim, J.K. Lee, H.J. Kim, J.C. Bae, J Kor Powd Met Inst. **12**, 406 (2005).
[15] D. Deporter, R. Todescan, P. Watson, M. Pharoah, R.M. Pilliar, G. Tomlinson, Int. J. Oral Maxillofac. Implants **16**, 527 (2001).
[16] D. Deporter, R.M. Pilliar, R. Todescan, P. Watson, M. Pharoah, Int. J. Oral Maxillofac. Implants **16**, 653 (2001).
[17] V. Amigo, M.D. Salvador, F. Romero, C. Solves, J.F. Moreno J. Mater. Process. Technol. **14**, 117 (2003).
[18] G.C. Li, Y. Wang, Y. Qin, Z.K. Zhang, J. Mater. Sci. **40**, 235 (2005).
[19] J. Eckert, J. Das, S. Pauly, C. Duhamel, J. Mater. Res. **22**, 285 (2007).
[20] C. Fan, R.T. Ott, T.C. Hufnagel, Appl. Phys. Lett. **81**, 1020 (2002).
[21] T.S. Srivatsan, B.G. Ravi, M. Petraroli, T.S. Sudarshan. Int. J. Ref. Met. Hard Mater. **20**, 181 (2002).
[22] Y.H. Zhao, X.Z. Liao, S. Cheng, E. Ma, Y.T. Zhu. Adv Mater. **18**, 2280 (2006).
[23] T. Jiao, L.J. Kecskes, T.C. Hufnagel, K.T. Ramesh. Metall Mater Trans A. **35A**, 3439 (2004).
[24] M.H. Lee, D.J. Sordelet. J Mater Res. **21**, 492 (2006).
[25] A. Leonhard, L.Q. Xing, M. Heilmaier, A. Gebert, J. Eckert J.L. Schultz, Nano Struct, Mat. **10**, 805 (1998).
[26] S.Y. Kim, B.K. Guem, M.H. Lee, B.S. Kim, J Kor Powd Met Inst. **20**, 33 (2013).
[27] C.W. Tang, C. Kuo, M.C. Kuo, C.B. Wang, S.H. Chien, Applied Catalysis A: general **309**, 37 (2006).

Received: 20 November 2014.